

On plate tectonics and ocean temperatures

Christian V  rard^{1,*} and J  n Veizer²

¹Department of Earth Sciences, University of Geneva, 13 Rue des Mara  chers, 1205 Geneva, Switzerland

²Department of Earth and Environmental Sciences, University of Ottawa, Ottawa, Ontario K1N 6N5, Canada

ABSTRACT

[REDACTED]

typical of diagenetic systems. Moreover, the Phanerozoic evolution of skeletal organisms enabled replication of the secular trend even for single-component samples, such as shells composed exclusively of the relatively diagenetically resistant low-Mg calcite (Fig. 1; Veizer et al., 1999). In addition, parallel secular trends, offset by their mineral-specific fractionation factors, have been documented also for siliceous (e.g., Perry, 1967; Knauth and Epstein, 1976; Kolodny and Epstein, 1976; Knauth and Lowe, 1978) and phosphatic (e.g., Longinelli and Nuti, 1968; Kolodny and Luz, 1991; Song et al., 2019)

INTRODUCTION

The advent of isotope geology as an empirical science evoked a hope for a tool that would enable estimation of the temperature of ancient oceans on geological time scales via measuring oxygen isotopic composition in ancient marine shells (Urey et al., 1951). Initially, the immediate success of this technique in Quaternary studies (Emiliani, 1955) appeared to justify these expectations, but subsequent results from ancient carbonate rocks (e.g., Baertshi, 1957; Degens and Epstein, 1962; Keith and Weber, 1964; Veizer and Hoefs, 1976) demonstrated large declines in calcite oxygen isotope values, $\delta^{18}\text{O}_c$, from $\sim 31\text{‰} \pm 2\text{‰}$ SMOW (Standard Mean Ocean Water) today to some $15\text{‰} \pm 5\text{‰}$ in the Archean, with about half of this shift attributable to Phanerozoic time (Fig. 1). Because post-depositional diagenetic alteration (Gross, 1964) or higher-temperature recrystallization of carbonate phases usually leads to ^{18}O depletion, the early consensus maintained that the secular trend is due principally to post-depositional resetting of the oxygen isotope signal, with the degree of shift proportional to the age of the samples (see Land [1995] versus Veizer [1995]). Yet, the amplitude of this shift exceeds the ranges

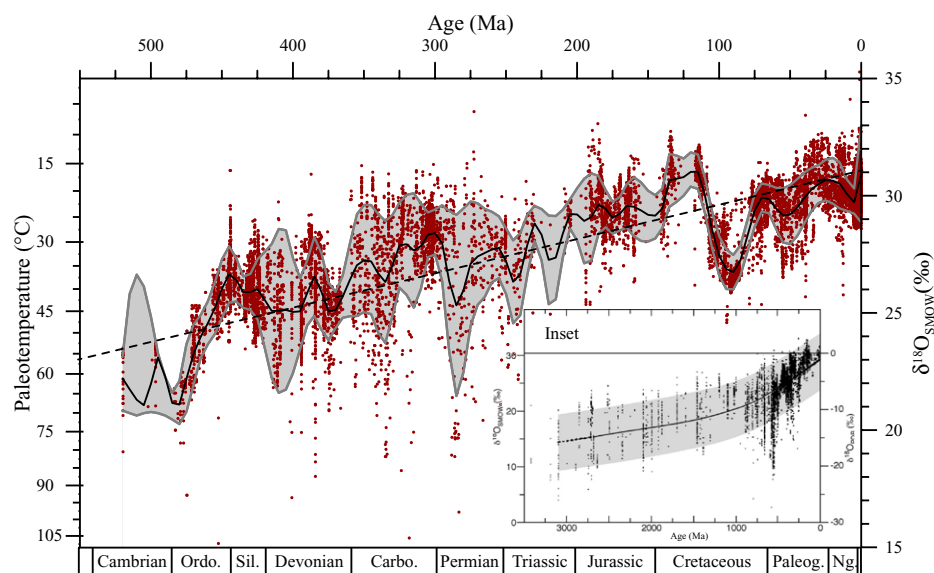


Figure 1. $\delta^{18}\text{O}_c$ (c—carbonate) data from Veizer and Prokoph (2015, their appendices) for the Phanerozoic (red dots). Because of the uneven distribution of 58,532 samples, a Gaussian moving average with a 5 m.y. window (comparable to the temporal resolution of stratigraphic biozones) has been applied (see the Data Repository [see footnote 1]) to calculate their means and associated 1σ intervals (gray area). Black curve is the spline function resampling these data. Dashed black line is a Phanerozoic linear trend (1‰ in $\delta^{18}\text{O}_c$ for every 72.7 m.y.; $R^2 = 92.5\%$). Apparent paleotemperatures are for information only. Inset: The extension (black dots) of the $\delta^{18}\text{O}_c$ trend, and associated cubic smoothing spline (black line with associated spread of values shaded in gray) to 3.5 b.y. of planetary history from Kasting et al. (2006). Geological time scale from the International Commission on Stratigraphy (Cohen et al., 2013; updated in 2018). SMOW—Standard Mean Ocean Water; Ordo.—Ordovician; Sil.—Silurian; Carbo.—Carboniferous; Paleog.—Paleogene; Ng.—Neogene; PDB—Peedee belemnite.

*E-mail: christian.verard@unige.ch

minerals and shells. All of this demonstrates that the $\delta^{18}\text{O}$ secular trends are primary features of the geologic record, where the secondary resetting phenomena contribute only superimposed scatter, mostly within the secular bands.

HYDROSPHERE-LITHOSPHERE COUPLING

On geological time scales, seawater $\delta^{18}\text{O}$ ($\delta^{18}\text{O}_{\text{sw}}$) is controlled by circulation of water through, and exchange of oxygen with, the silicate rocks of the crust and upper mantle. In modern oceans, seawater reacting with silicate minerals in hydrothermal systems at temperatures exceeding some 350 °C becomes enriched in ^{18}O , and at colder temperatures, depleted in this isotope. The $\delta^{18}\text{O}_{\text{sw}}$ at any given time is therefore believed to represent a balancing act of these competing fluxes. The models that simulate secular oxygen isotopic evolution of seawater vary in complexity, with the number of fluxes and related phenomena increasing from 4 to 17 from the older to the younger attempts. They disagree in outcome, with some authors arguing that $\delta^{18}\text{O}_{\text{sw}}$ over the entirety of geologic history was buffered at near-modern values of $\sim 0\text{‰}$ SMOW (Muehlenbachs and Clayton, 1976; Holland, 1984; Gregory and Taylor, 1981; Muehlenbachs, 1986; Gregory, 1991; Jean-Baptiste et al., 1997; Lécuyer and Allemand, 1999), while others proposed model adjustments that contested this supposition (Walker and Lohmann, 1989; Wallmann, 2001, 2004; Kasting et al., 2006; Jafriés et al., 2007). Regardless of the outcome, all have accepted the notion that the principal transfer of ^{18}O between hydrosphere and lithosphere is achieved via hydrothermal systems associated with oceanic ridges and their flanks, along the lines of the model originally proposed by Muehlenbachs and Clayton (1976) where the “buffering” is attributed to the reversal of oxygen isotope alteration signature in modern oceanic crust, and its ancient analogues, at the depth of the 350 °C thermocline.

Due to this assumption, a multitude of studies published over the last four decades inadvertently had to resort to violation of the actualistic principle by invoking geologically and/or ecologically improbable (Storch et al., 2014; Veizer and Prokoph, 2015; Reddin et al., 2018) hot ancient oceans. While accepting the conceptual validity of the Muehlenbachs and Clayton (1976) model, we argue that it is not the claimed or potential masses of altered rocks but rather the fluxes of water that circulate through the respective temperature domains that modulate ocean chemistry.

WATER FLUXES

Today, the energy flux from the interior of the earth is estimated to be ~ 47 TW (Davies and Davies, 2010), with three-quarters dissipated via oceanic crust, and 15% associated directly

with hydrothermal systems on submarine ridges and their flanks (Stein and Stein, 1994). Constraints of this energy budget imply that the hot-temperature (axial and flank-entrained) water flux is $\sim 48 \times 10^{13}$ kg/yr, while the off-axis low-temperature one is $1\text{--}4 \times 10^{16}$ kg/yr (German and Von Damm, 2006, their table 1). The cold flux swamps the hot one by two orders of magnitude, and more if the interaction over the entire ocean floor is taken into account (Coogan and Gillis, 2018). Attempting to close the gap by invoking ^{18}O -enriched high-temperature reflux at the opposite end of plate tectonic conveyor belt is not a solution because the water flux due to subduction magmatism, estimated at $\sim 10^{11}\text{--}10^{12}$ kg/yr (Wallace, 2005; Parai and Mukhopadhyay, 2012), is short by at least four orders of magnitude. This huge discrepancy casts serious doubts on the prime assumption of all models based on a balance of countervailing hydrothermal fluxes. For specific components and isotopes, the balance can be claimed via kinetics of alteration that is exponentially scaled to temperature (Cole and Chakraborty, 2001), but this is of little import for oxygen isotopes when practically 99% of the entire rock-water exchange in the oceanic crust proceeds within the ^{18}O -consuming cold-temperature hydrothermal regime. Considering that this massive low-temperature flux, essential also for major and trace element budgets of the oceans (Staudigel, 2003; Coogan and Gillis, 2018), can theoretically recycle an equivalent of the modern ocean water mass (1.4×10^{21} kg) in $\sim 10^5$ yr, it is difficult to escape the conclusion that ^{18}O is stripped from water and transported into the mantle via subduction of altered oceanic crust. Moreover, the original hydrosphere outgassed by the planet would have acquired $\delta^{18}\text{O}_{\text{sw}}$ of the chondritic bulk earth, $\sim 7\text{‰} \pm 1\text{‰}$ SMOW, comparable to empirical values for “primordial”, “juvenile”, or “magmatic” waters (Hoefs, 1997). Its subsequent evolution would then have to have led somehow to its present-day value of 0‰ SMOW. Our scenario can provide an explanation both for $\delta^{18}\text{O}$ of modern seawater and for even greater ^{18}O depletion expected for times of more active tectonics in the geological past. The pervasive silicification (chertification) and carbonation overprint of ancient greenstone lithologies, such as the 3.4 Ga Onverwacht group (Knauth and Lowe, 1978), is the vestigial relic of such extensive hydrothermalism on the young Earth.

In summary, unless the high-temperature hydrothermal cells prove to be grossly underestimated, it appears likely that the long-term secular evolution of $\delta^{18}\text{O}_{\text{sw}}$ has been modulated chiefly by the declining off-axis low-temperature alteration flux that has gradually diminished its excess over the countervailing high-temperature phenomena, ^{18}O buildup toward the present-day value of 0‰ SMOW being an outcome. ^{18}O -depleted ancient

oceans were therefore the norm, with the isotopic depletion gradually diminishing as the internal energy of the planet wanes, potentially even reverting to a “primordial” value of $\sim 7\text{‰}$ SMOW with future cessation (e.g., Vérard et al., 2015a) of plate tectonic activity. The secular trend in $\delta^{18}\text{O}_c$ (Fig. 1 inset) is an empirical reflection of such evolution.

ALTERNATE SCENARIO TO THE HOT OCEAN SCENARIO

Our interpretation could potentially be negated by independent *direct*—as opposed to indirectly inferred—paleotemperature estimates, such as from “clumped isotopes”, that are apparently consistent with the hot-ocean alternative. For example, early Paleozoic phosphatic shells (Bergmann et al., 2018) yield apparent temperatures of 29–52.3 °C. Note, however, that the calculated $\delta^{18}\text{O}_{\text{sw}}$ for even the coldest (29 °C) *shell* sample is then $+2.3\text{‰}$ SMOW, and such or even more positive values (usually a signal of alteration) are the norm, not exceptions (Bergmann et al., 2018, their table 2 and figures 10 and 11). Because the most likely cause for positive shift in $\delta^{18}\text{O}$ of open-ocean seawater is the storage of ^{16}O in massive ice caps, the temperatures derived from clumped isotopes require that the Ordovician oceans not only were hot but apparently coexisted with ice caps (Finnegan et al., 2011) that were twice the size of those of the Last Glacial Maximum, a pure *ad hoc* postulate. The need to resort to such an exotic interpretation argues that clumped-isotope systematics, unquestionably a desirable and promising new tool, is still a technique in developmental stages, and its advantages and limitations have yet to be established. Note also that the clumped-isotope thermometer routinely yields elevated temperatures, even for “pristine” modern shells (Bergmann et al., 2018, their figure 5; Zaarur et al., 2011; Wang et al., 2016). At this stage, the meaning of the “temperature” estimates by this technique is still open to debate, as is the resistance of this isotope system to solid-state atomic-scale reordering down to low diagenetic temperatures, the stage at which newly deposited shells that initially harbor many impurities and dislocations are particularly vulnerable (Veizer and Prokoph, 2015). The need for reinterpretation of the geological context by invoking exotic calcification, paleoenvironmental and geological phenomena, may not then arise.

PLATE TECTONIC DRIVER

Our scenario posits a relationship between plate tectonics and oxygen isotopic composition of seawater where, over geologic history, the decline in tectonic activity retards the transfer of ^{18}O from seawater into the subducting oceanic crust, thus generating the progressively heavier $\delta^{18}\text{O}_{\text{sw}}$ and $\delta^{18}\text{O}_c$. With our resolution of 5 m.y. (see the caption of Figure 1 and the

GSA Data Repository¹), the proposition should theoretically be tested over a 10^7 – 10^9 yr time span, but the record of desired quality for oxygen isotopes is presently available only for the Phanerozoic (Fig. 1), and for the oceanic crust, obliterated by the Jurassic, it is shorter still. For the latter, therefore, we have to base our discussion on model evaluation of proxy data. The UNIL plate tectonic model (developed by the geodynamic group at the University of Lausanne, Switzerland; <https://www.unil.ch/iste/fr/home.html>) over three decades (Stampfli and Borel, 2002; Hochard, 2008; V  rard et al., 2015a, 2015b; V  rard, 2018) reconstructed 100% of Earth's surface back to the Neoproterozoic. Following the precepts of plate tectonics, the model projected the positions of 1046 "geodynamic units" into 48 time slices, which in turn has enabled calculation of derivative temporal parameters, such as the ages and rates of generation and destruction of oceanic crust (V  rard et al., 2015a, 2015b). Consistent with our scenario, the results indeed point to decelerating tectonic activity, with the first-order linear "tectonic activity" index (V  rard et al., 2015a) declining by a factor of 2.4, from ~ 8.5 to 3.5 km^2/yr over the Phanerozoic (Fig. 2), coincident with $\sim 8\text{‰} \pm 2\text{‰}$ rise in $\delta^{18}\text{O}$ (Fig. 1). Extrapolating this gradient into the Archean, the $\delta^{18}\text{O}$ of $\sim 15\text{‰}$ (Fig. 1 inset) then translates into a factor of 4.5 ± 1.5 , in reasonable agreement with model estimates for the declining heat-flow regime of the Earth (Condie, 2003, his figure 5.1).

PHANEROZOIC OCEAN TEMPERATURE

Subtraction of the long-term component from the secular $\delta^{18}\text{O}_c$ trend yields a detrended pattern of residual oscillations on 10^7 yr time scales (Fig. 3). Its cross-correlation with the 10^7 yr oscillations in the detrended plate-tectonic signal is, however, poor ($R^2 = 48.5\%$), suggesting that on time scales shorter than 10^8 yr, tectonics impacts the oxygen isotope signals only marginally, if at all. The superimposed higher-order $\delta^{18}\text{O}_c$ oscillations (Fig. 3) are therefore more likely proxy signals of Phanerozoic climate history. The detrended pattern in Figure 3 is a stationary time series with oscillations at a 10^7 yr frequency and an overall amplitude of 5‰ , or $\sim 20^\circ\text{C}$. If climate related, the pattern may be generated, singly or in concert, by ice-volume (icehouse-greenhouse) effects or by temperature of seawater. Because the ice-volume correction of $\delta^{18}\text{O}_{sw}$ can account for only a small portion, $<1\text{‰}$ or $<4^\circ\text{C}$ (Werner et al., 2016), of the observed

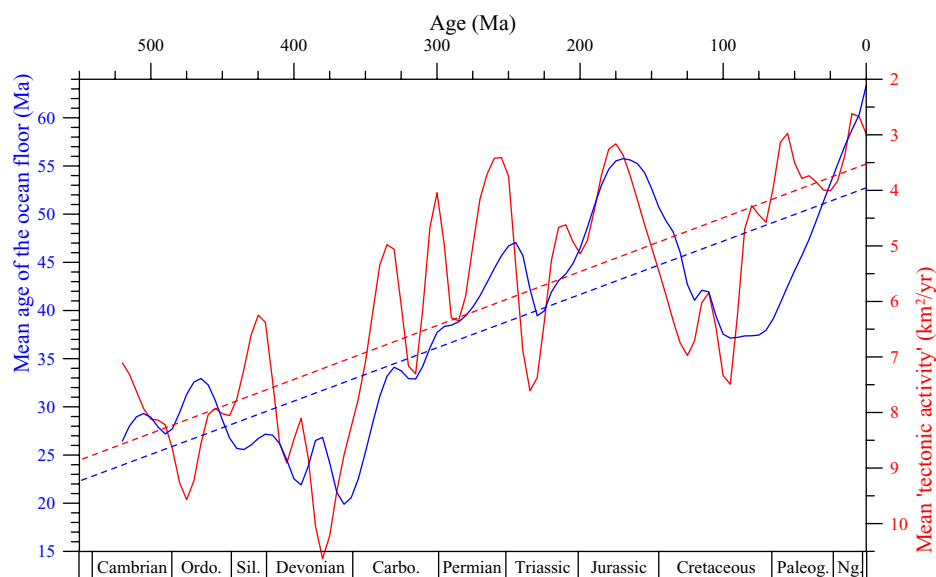


Figure 2. Global temporal parameters derived from the UNIL plate tectonic model (developed by the geodynamic group at the University of Lausanne, Switzerland; V  rard et al., 2015a) with the same resolution as isotope data (5 m.y.): global mean age of the ocean floor (blue curve) and global mean "tectonic activity" (red curve). The slopes of the associated first-order linear trends (dashed lines) are significant at the 99% confidence level (Mann-Kendall trend test; see the Data Repository [footnote 1]). The index of mean "tectonic activity" averages the mean accretion rate at mid-oceanic ridges and the mean subduction rate at trenches (V  rard et al., 2015a), which differ marginally in detail because the UNIL model excludes from those rates the areas of rifting and collision zones (i.e., in continental areas). Note that the y-axis for "tectonic activity" is inverted. Geological time scale from the International Commission on Stratigraphy (Cohen et al., 2013; updated in 2018). Ordo.—Ordovician; Sil.—Silurian; Carbo.—Carboniferous; Paleog.—Paleogene; Ng.—Neogene.

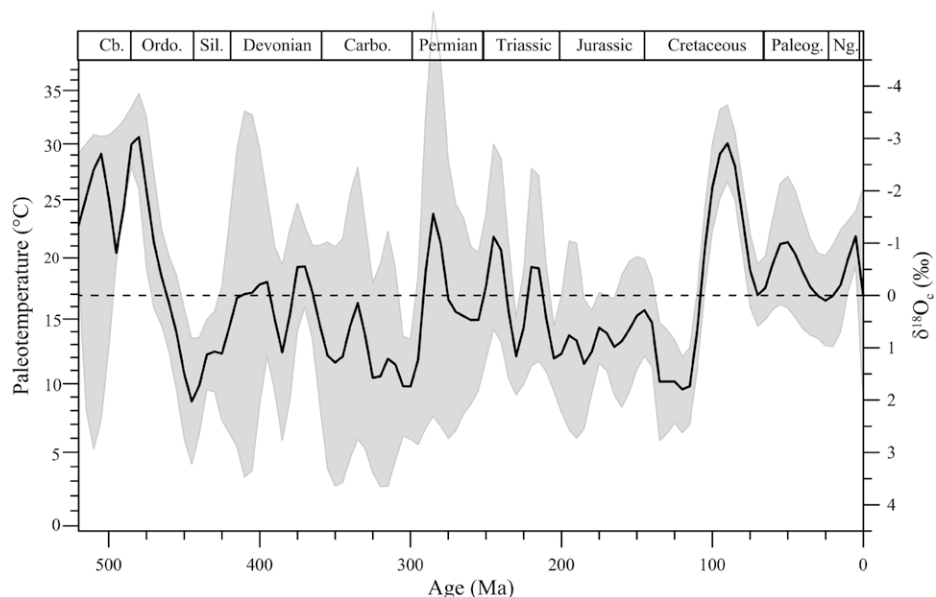


Figure 3. Linearly detrended $\delta^{18}\text{O}_c$ (c—carbonate) data (black line; $\pm 1\sigma$ in gray; from the same data as per Figure 1). Note that the y-axis for the $\delta^{18}\text{O}_c$ data is inverted to project increases in temperature upward. Geological time scale from the International Commission on Stratigraphy (Cohen et al., 2013; updated in 2018). Cb.—Cambrian; Ordo.—Ordovician; Sil.—Silurian; Carbo.—Carboniferous; Paleog.—Paleogene; Ng.—Neogene.

amplitudes, seawater temperature variations are the most likely culprit. The paleotemperature pattern for low-latitude shallow Phanerozoic oceans (Fig. 3) is a stationary time series, oscillating between 10 and 30°C around a baseline

of 17°C , well within the range of temperatures of modern seawater (Abraham et al., 2013). Note nevertheless that our database, resampled with 5 m.y. resolution, cannot exclude the possibility of more extreme events at smaller temporal and

¹GSA Data Repository item 2019319, all resampled data (every 5 m.y.) and associated statistics, is available online at <http://www.geosociety.org/datarepository/2019/>, or on request from editing@geosociety.org.

spatial scales. Note also that potential inclusion of somewhat altered samples, not recognized by our screening procedures, may bias the means toward warmer values because alteration almost invariably results in ^{18}O depletion. Considering the huge size of our database, the impact on the mean values for most subpopulations with a large number of samples is minimal. This may, nevertheless, be of concern for time intervals that have a large spread of values and large O^{18} -depleted tail. The early Permian peak (Fig. 3) may be a potential candidate.

Phanerozoic climate reconstructions based on geological and biological climate indicators (Frakes et al., 2003; Scotese et al., 2016), essential for “ground truth” validation of proxy paleothermometry, are by their nature only qualitative to semiquantitative descriptive summaries that are not easily translatable into numerical values. The two clearly dominant isotope temperature peaks, in the Cambrian to early Ordovician and the middle to Late Cretaceous (Fig. 3), are in good agreement with geological paleoclimate reconstructions. The less-pronounced oscillations—the cooling in the Ordovician, the warm mid-Paleozoic, the cooling during the Carboniferous, the hot late Permian and early Triassic followed by an overall cooling trend from the Triassic into the early Cretaceous, the warm late Cretaceous turning into another overall cooling trend during the Cenozoic—are all in broad agreement with interpretations based on field paleoclimate indicators, particularly if the uncertainties in temporal correlations of the two approaches are taken into account. Nevertheless, even though the general agreement of the two approaches—oxygen isotope thermometry and field observations—is encouraging, we wish to emphasize that translation of isotope amplitudes into temperature still requires more precise verification and calibration.

In summary, the oxygen isotope signal of past seawater appears to be firmly embedded in the larger picture of planetary evolution driven by declining internal heat dissipation over the eons of geologic time. The secular trends for $\delta^{18}\text{O}$ in marine sediments (carbonates, cherts, phosphates) are proxy signals of this evolution, and future empirical advances may enable application of the approach beyond the Phanerozoic, into the hazy Precambrian storage of some four-fifths of the planetary history.

ACKNOWLEDGMENTS

We appreciate the helpful and constructive comments of Jochen Hoefs, Kent Condie, and an anonymous reviewer. Veizer acknowledges financial support from the G.G. Hatch Fund at the University of Ottawa, Canada.

REFERENCES CITED

Abraham, J.P., et al., 2013, A review of global ocean temperature observations: Implications for ocean

heat content estimates and climate change: *Reviews of Geophysics*, v. 51, p. 450–483, <https://doi.org/10.1002/rog.20022>.

Baertschi, P., 1957, Messung und Deutung relativer Häufigkeitsvariationen von ^{18}O und ^{13}C in Karbonatgesteinen und Mineralien: *Schweizerische Mineralogische und Petrographische Mitteilungen*, v. 37, p. 73–152.

Bergmann, K.D., Finnegan, S., Creel, R., Eiler, J.M., Hughes, N.C., Popov, L.E., and Fisher, W.W., 2018, A paired apatite and calcite clumped isotope thermometry approach to estimating Cambro-Ordovician seawater temperatures and isotopic composition: *Geochimica et Cosmochimica Acta*, v. 224, p. 18–41, <https://doi.org/10.1016/j.gca.2017.11.015>.

Cohen, K.M., Finney, S.C., Gibbard, P.L., and Fan, J.-X., 2013, The ICS International Chronostratigraphic Chart: Episodes, v. 36, p. 199–204 (updated version 2018/08).

Cole, D.R., and Chakraborty, A., 2001, Rates and mechanisms of isotopic exchange: *Reviews in Mineralogy and Geochemistry*, v. 43, p. 83–223, <https://doi.org/10.2138/gsrmg.43.1.83>.

Condie, K.C., 2003, *Plate Tectonics and Crustal Evolution*, 4th Edition: Oxford, UK, Butterworth-Heinemann, 282 p.

Coogan, L.A., and Gillis, K.M., 2018, Low-temperature alteration of the seafloor: Impact on ocean chemistry: *Annual Review of Earth and Planetary Sciences*, v. 46, p. 21–45, <https://doi.org/10.1146/annurev-earth-082517-010027>.

Davies, J.H., and Davies, D.R., 2010, Earth's surface heat flux: *Solid Earth*, v. 1, p. 5–24, <https://doi.org/10.5194/se-1-5-2010>.

Degens, E.T., and Epstein, S., 1962, Relationship between $^{18}\text{O}/^{16}\text{O}$ ratios in coexisting carbonate, cherts, and diatomites: *Bulletin of the American Association of Petroleum Geologists*, v. 46, p. 534–542, <https://doi.org/10.1306/BC743841-16BE-11D7-8645000102C1865D>.

Emiliani, C., 1955, Pleistocene temperatures: *The Journal of Geology*, v. 63, p. 538–578, <https://doi.org/10.1086/626295>.

Finnegan, S., Bergmann, K., Eiler, J.M., Jones, D.S., Fike, D.A., Eisenman, I., Hughes, N.C., Tripathi, A.K., and Fischer, W.W., 2011, The magnitude and duration of Late Ordovician–Early Silurian glaciation: *Science*, v. 331, p. 903–906, <https://doi.org/10.1126/science.1200803>.

Frakes, L.A., Francis, J.E., and Syktus, J., 2003, *Climate Modes of the Phanerozoic: The History of the Earth's Climate over the Past 600 Million Years*: Cambridge, UK, Cambridge University Press, 288 p.

German, C.R., and Von Damm, K.L., 2006, Hydrothermal processes, in Elderfield, H., ed., *Treatise on Geochemistry*, Volume 6: The Oceans and Marine Geochemistry: Amsterdam, Elsevier, p. 181–222, <https://doi.org/10.1016/B0-08-043751-6/06109-0>.

Gregory, R.T., 1991, Oxygen isotope history of seawater revisited: Timescales and boundary event changes in the oxygen isotope composition of seawater, in Taylor, H.P. Jr., et al., eds., *Stable Isotope Geochemistry: A Tribute to Samuel Epstein*: Geochemical Society Special Publication 3, p. 65–76.

Gregory, R.T., and Taylor, H.P.J., 1981, An oxygen isotope profile in a section of Cretaceous oceanic crust, Samail Ophiolite, Oman: Evidence for $\delta^{18}\text{O}$ buffering of the ocean by deep (>5 km) seawater-hydrothermal circulation at mid-ocean ridges: *Journal of Geophysical Research*, v. 86, p. 2737–2755, <https://doi.org/10.1029/JB086iB04p02737>.

Gross, M.G., 1964, Variations in the $^{18}\text{O}/^{16}\text{O}$ and $^{13}\text{C}/^{12}\text{C}$ ratios of diagenetically altered limestones in the

Bahama Islands: *The Journal of Geology*, v. 72, p. 170–194, <https://doi.org/10.1086/626975>.

Hochard, C., 2008, *GIS and geodatabases application to global scale plate tectonics modelling* [Ph.D. thesis]: Lausanne, Switzerland, University of Lausanne, Faculté des Sciences et de l'Environnement, 164 p.

Hoefs, J., 1997, *Stable Isotope Geochemistry*: Berlin, Springer, 203 p., <https://doi.org/10.1007/978-3-662-03377-7>.

Holland, H.D., 1984, *The Chemical Evolution of the Atmosphere and Oceans*: Princeton, New Jersey, Princeton University Press, 582 p.

Jaffrés, J.B.D., Shields, G.A., and Wallmann, K., 2007, The oxygen isotope evolution of seawater: A critical review of a long-standing controversy and an improved geological water cycle model for the past 3.4 billion years: *Earth-Science Reviews*, v. 83, p. 83–122, <https://doi.org/10.1016/j.earscirev.2007.04.002>.

Jean-Baptiste, P., Charlou, J.L., and Stievenard, M., 1997, Oxygen isotope study of mid-ocean ridge hydrothermal fluids: Implication for the ^{18}O budget of the oceans: *Geochimica et Cosmochimica Acta*, v. 61, p. 2669–2677, [https://doi.org/10.1016/S0016-7037\(97\)00090-2](https://doi.org/10.1016/S0016-7037(97)00090-2).

Kasting, J.F., Howard, M.T., Wallmann, K., Veizer, J., Shields, G., and Jaffrés, J., 2006, Paleoclimates, ocean depth, and the oxygen isotopic composition of seawater: *Earth and Planetary Science Letters*, v. 252, p. 82–93, <https://doi.org/10.1016/j.epsl.2006.09.029>.

Keith, M.L., and Weber, J.N., 1964, Carbon and oxygen isotopic composition of selected limestones and fossils: *Geochimica et Cosmochimica Acta*, v. 28, p. 1787–1816, [https://doi.org/10.1016/0016-7037\(64\)90022-5](https://doi.org/10.1016/0016-7037(64)90022-5).

Knauth, L.P., and Epstein, S., 1976, Hydrogen and oxygen isotope ratios in nodular and bedded cherts: *Geochimica et Cosmochimica Acta*, v. 40, p. 1095–1108, [https://doi.org/10.1016/0016-7037\(76\)90051-X](https://doi.org/10.1016/0016-7037(76)90051-X).

Knauth, L.P., and Lowe, D.R., 1978, Oxygen isotope geochemistry of cherts from the Onverwacht group (3.4 billion years), Transvaal, South Africa, with implications for secular variations in the isotopic composition of cherts: *Earth and Planetary Science Letters*, v. 41, p. 209–222, [https://doi.org/10.1016/0012-821X\(78\)90011-0](https://doi.org/10.1016/0012-821X(78)90011-0).

Kolodny, Y., and Epstein, S., 1976, Stable isotope geochemistry of deep sea cherts: *Geochimica et Cosmochimica Acta*, v. 40, p. 1195–1209, [https://doi.org/10.1016/0016-7037\(76\)90155-1](https://doi.org/10.1016/0016-7037(76)90155-1).

Kolodny, Y., and Luz, B., 1991, Oxygen isotopes in phosphates of fossil fish—Devonian to Recent, in Taylor, H.P. Jr., et al., eds., *Stable Isotope Geochemistry: A Tribute to Samuel Epstein*: Geochemical Society Special Publication 3, p. 105–119.

Land, L.S., 1995, Comment on “Oxygen and carbon isotopic composition of Ordovician brachiopods: Implications for coeval seawater” by H. Qing and J. Veizer: *Geochimica et Cosmochimica Acta*, v. 59, p. 2843–2844, [https://doi.org/10.1016/0016-7037\(95\)00176-Z](https://doi.org/10.1016/0016-7037(95)00176-Z).

Lécuyer, C., and Allemand, P., 1999, Modelling of oxygen isotope evolution of seawater: Implications for the climate interpretation of the $\delta^{18}\text{O}$ of marine sediments: *Geochimica et Cosmochimica Acta*, v. 63, p. 351–361, [https://doi.org/10.1016/S0016-7037\(98\)00277-4](https://doi.org/10.1016/S0016-7037(98)00277-4).

Longinelli, A., and Nuti, S., 1968, Oxygen isotopic composition of phosphorites from marine formations: *Earth and Planetary Science Letters*, v. 5, p. 13–16, [https://doi.org/10.1016/S0012-821X\(68\)80003-2](https://doi.org/10.1016/S0012-821X(68)80003-2).

- Muehlenbachs, K., 1986, Alteration of oceanic crust and the ^{18}O history of seawater, in Valley, J.W., et al., eds., *Stable Isotopes in High Temperature Geological Processes: Reviews in Mineralogy and Geochemistry*, v. 16, p. 425–444, <https://doi.org/10.1515/9781501508936-017>.
- Muehlenbachs, K., and Clayton, R.N., 1976, Oxygen isotopic composition of the oceanic crust and its bearing on seawater: *Journal of Geophysical Research*, v. 81, p. 4365–4369, <https://doi.org/10.1029/JB081i023p04365>.
- Parai, R., and Mukhopadhyay, S., 2012, How large is a subducted water flux? New constraints on mantle regassing rates: *Earth and Planetary Science Letters*, v. 317–318, p. 396–406, <https://doi.org/10.1016/j.epsl.2011.11.024>.
- Perry, E.C., 1967, The oxygen isotope chemistry of ancient cherts: *Earth and Planetary Science Letters*, v. 3, p. 62–66, [https://doi.org/10.1016/0012-821X\(67\)90012-X](https://doi.org/10.1016/0012-821X(67)90012-X).
- Reddin, C.J., Kocsis, Á.T., and Kiessling, W., 2018, Marine invertebrate migrations trace climate change over 450 million years: *Global Ecology and Biogeography*, v. 27, p. 704–713, <https://doi.org/10.1111/geb.12732>.
- Scotese, R.S., Boucot, A.J., and Xu, C., 2016, *Atlas of Phanerozoic climatic zones (Mollweide projection)*, Volumes 1–6: PALEOMAP Project Paleogeographic Atlas for ArcGIS: Evanston, Illinois, PALEOMAP Project, 32 p.
- Song, H., Wignall, P.B., Song, H., Dai, X., and Chu, D., 2019, Seawater temperature and dissolved oxygen over the past 500 million years: *Journal of Earth Science*, v. 30, p. 236–243, <https://doi.org/10.1007/s12583-018-1002-2>.
- Stampfli, G.M., and Borel, G.D., 2002, A plate tectonic model for the Paleozoic and Mesozoic constrained by dynamic plate boundaries and restored synthetic oceanic isochrons: *Earth and Planetary Science Letters*, v. 196, p. 17–33, [https://doi.org/10.1016/S0012-821X\(01\)00588-X](https://doi.org/10.1016/S0012-821X(01)00588-X).
- Staudigel, H., 2003, Hydrothermal alteration processes in the oceanic crust, in Rudnick, R.L., *Treatise on Geochemistry*, Volume 3: The Crust: Amsterdam, Elsevier, p. 511–535, <https://doi.org/10.1016/B00-08-043751-6/03032-2>.
- Stein, C.A., and Stein, S., 1994, Constraints on hydrothermal heat flux through the oceanic lithosphere from global heat flow: *Journal of Geophysical Research*, v. 99, p. 3081–3095, <https://doi.org/10.1029/93JB02222>.
- Storch, D., Menzel, L., Frickenhaus, S., and Pörtner, H.-O., 2014, Climate sensitivity across marine domains of life: Limits to evolutionary adaptation shape species interaction: *Global Change Biology*, v. 20, p. 3059–3067, <https://doi.org/10.1111/gcb.12645>.
- Urey, H.C., Lowenstam, H.A., Epstein, S., and McKinnin, C.R., 1951, Measurement of paleotemperatures and temperatures of the Upper Cretaceous of England, Denmark, and the southern United States: *Geological Society of America Bulletin*, v. 62, p. 399–416, [https://doi.org/10.1130/0016-7606\(1951\)62\[399:MOPATO\]2.0.CO;2](https://doi.org/10.1130/0016-7606(1951)62[399:MOPATO]2.0.CO;2).
- Veizer, J., 1995, Reply to the Comment by L.S. Land on “Oxygen and carbon isotopic composition of Ordovician brachiopods: Implications for coeval seawater”: *Geochimica et Cosmochimica Acta*, v. 59, p. 2845–2846, [https://doi.org/10.1016/0016-7037\(95\)00177-2](https://doi.org/10.1016/0016-7037(95)00177-2).
- Veizer, J., and Hoefs, J., 1976, The nature of $^{18}\text{O}/^{16}\text{O}$ and $^{13}\text{C}/^{12}\text{C}$ secular trends in sedimentary carbonate rocks: *Geochimica et Cosmochimica Acta*, v. 40, p. 1387–1395, [https://doi.org/10.1016/0016-7037\(76\)90129-0](https://doi.org/10.1016/0016-7037(76)90129-0).
- Veizer, J., and Prokoph, A., 2015, Temperature and oxygen isotopic composition of Phanerozoic oceans: *Earth-Science Reviews*, v. 146, p. 92–104, <https://doi.org/10.1016/j.earscirev.2015.03.008>.
- Veizer, J., et al., 1999, $^{87}\text{Sr}/^{86}\text{Sr}$, $\delta^{13}\text{C}$ and $\delta^{18}\text{O}$ evolution of Phanerozoic seawater: *Chemical Geology*, v. 161, p. 59–88, [https://doi.org/10.1016/S0009-2541\(99\)00081-9](https://doi.org/10.1016/S0009-2541(99)00081-9).
- Vérard, C., 2018, Plate tectonic modelling: Review and perspectives: *Geological Magazine*, v. 156, p. 208–241, <https://doi.org/10.1017/S0016756817001030>.
- Vérard, C., Hochard, C., Baumgartner, P.O., and Stampfli, G.M., 2015a, Geodynamic evolution of the Earth over the Phanerozoic: Plate tectonic activity and palaeoclimatic indicators: *Journal of Palaeogeography*, v. 4, p. 167–188, <https://doi.org/10.3724/SPJ.1261.2015.00072>.
- Vérard, C., Hochard, C., Baumgartner, P.O., and Stampfli, G.M., 2015b, 3D palaeogeographic reconstructions of the Phanerozoic versus sea-level and Sr-ratio variations: *Journal of Palaeogeography*, v. 4, p. 64–84, <https://doi.org/10.3724/SPJ.1261.2015.00068>.
- Walker, J.G.C., and Lohmann, K.C., 1989, Why the oxygen isotopic composition of seawater changes through time: *Geophysical Research Letters*, v. 16, p. 323–326, <https://doi.org/10.1029/GL016i004p00323>.
- Wallace, P.J., 2005, Volatiles in subduction zone magmas: Concentrations and fluxes based on melt inclusions and volcanic gas data: *Journal of Volcanology and Geothermal Research*, v. 140, p. 217–240, <https://doi.org/10.1016/j.jvolgeores.2004.07.023>.
- Wallmann, K., 2001, The geological water cycle and the evolution of marine $\delta^{18}\text{O}$ values: *Geochimica et Cosmochimica Acta*, v. 65, p. 2469–2485, [https://doi.org/10.1016/S0016-7037\(01\)00603-2](https://doi.org/10.1016/S0016-7037(01)00603-2).
- Wallmann, K., 2004, Impact of atmospheric CO_2 and galactic cosmic radiation on Phanerozoic climatic change and marine $\delta^{18}\text{O}$ record: *Geochemistry Geophysics Geosystems*, v. 5, Q06004, <https://doi.org/10.1029/2003GC000683>.
- Wang, X., Cui, L., Zhai, J., and Ding, Z., 2016, Stable and clumped isotopes in shell carbonates and land snails *Cathaica* sp. and *Bradybaena* sp. in north China and implication for ecophysiological characteristics and paleoclimate studies: *Geochemistry Geophysics Geosystems*, v. 17, p. 219–231, <https://doi.org/10.1002/2015GC006182>.
- Werner, M., Haese, B., Xu, X., Zhang, X., Butzin, M., and Lohmann, G., 2016, Glacial-interglacial changes in H_2^{18}O , HDO and deuterium excess—Results from the fully coupled ECHAMS/MPI-OM Earth system model: *Geoscientific Model Development*, v. 9, p. 647–670, <https://doi.org/10.5194/gmd-9-647-2016>.
- Zaarur, S., Olack, G., and Affek, H.P., 2011, Paleoenvironmental implication of clumped isotopes in land snail shells: *Geochimica et Cosmochimica Acta*, v. 75, p. 6859–6869, <https://doi.org/10.1016/j.gca.2011.08.044>.

Printed in USA